Systems & Control Letters 203 (2025) 106164

Contents lists available at ScienceDirect

Systems & Control Letters

journal homepage: www.elsevier.com/locate/sysconle

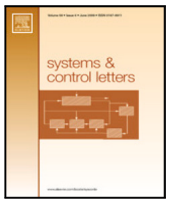

On the analysis of qualitative Nyquist plots

Davide Tebaldi *, Roberto Zanasi

University of Modena and Reggio Emilia, Via Pietro Vivarelli 10 - int. 1, Modena, 41125, Italy

ARTICLE INFO

Keywords:
Nyquist plots
Frequency response function
Frequency analysis
Graphical analysis
Qualitative Nyquist plot construction

ABSTRACT

A powerful tool in control and systems engineering is represented by Nyquist plots, for which a qualitative representation often gives a clearer visualization of the frequency response function that is typically not given by computer programs, especially if portions of the Nyquist plot extend to infinity. This letter addresses the graphical analysis of the frequency response function, with the objective of enhancing the procedure for the qualitative construction of Nyquist plots. Several results supported by analytical proofs are derived for what concerns the low and high frequency behavior, which enable to improve the qualitative construction of Nyquist plots in the vicinity of the initial and final points.

1. Introduction

Nyquist plots are one of the possible graphical representations of the frequency response function [1]. They have a large variety of different applications in the field of control theory, including the Nyquist stability criterion [2–5] for linear systems and the stability analysis of nonlinear systems using criteria such as the Circle criterion [6], the Popov criterion [6], or the describing function method [7]. Furthermore, Nyquist plots are also employed to perform the passivity analysis of physical systems [6], and to design lead/lag networks using the concept of admissible domain [8]. Nyquist plots also find application in several other fields, including the medical one as in [9], where they are employed within an algorithm that recognizes different types of swallowing events, which is used for screening and treatment of dysphagia. In [10], Nyquist plots are used for the thermal characterization of electronic packages, while a method based on the use of Nyquist plots to relax linear matrix inequalities conservatism for robust mechatronics synthesis is proposed in [11].

For what concerns the construction of Nyquist plots, an interesting feature is described in [12], showing that many Nyquist plots can be associated with characteristic curves on the complex plane. However, whenever a detailed and punctual representation of Nyquist plots is desired, their construction is typically addressed making use of computer aided control system design software, such as the Control System Toolbox available in the MATLAB/Simulink environment [13], the LabVIEW software [14], and others. However, the reading of the resulting Nyquist plots may not be easy, because of the large range in magnitude that can result when spanning a wide range of frequency. Following the same principle employed for Bode plots, some works employ the logarithmic scale for the magnitude representation [15] which, however, still require the use of computer aided control system design software and to arbitrary set the minimum magnitude value to be represented.

A qualitative representation is often sufficient to extract the desired features of the Nyquist plot. The typical approaches for constructing Nyquist plots require a large amount of calculations [1,16,17] and are essentially based on the analysis of the frequency response function at low and high frequencies. In [18], a revised version of the method for plotting qualitative Nyquist plots was proposed, based on the calculation of two novel parameters Δ_τ and Δ_p allowing to improve the Nyquist plot representation at low and high frequencies, with the specific objective of discriminating whether the Nyquist plot is leading or lagging compared to the initial and final phases, respectively. This procedure allows to enhance the comprehension of the plots given by computer aided control system design software. However, the proposed procedure did not consider in detail the cases $\Delta_\tau = 0$ and $\Delta_p = 0$. Furthermore, these two parameters only encompass information about the phase, without giving information about the modulus of the Nyquist plot in the vicinity of the initial and final points.

In the present letter, we extend the work in [18] by providing the following new contributions: (1) a much deeper frequency response analysis at low frequency. In detail, a Taylor series expansion truncated at the first order was employed in [18], while all the Taylor series expansion terms are taken into account in the present work, by also providing two properties for the recursive calculation of the Taylor coefficients. (2) the generalization of the extended low-frequency response analysis to the high-frequency case, providing dual results; (3) the generalization of the previous parameters Δ_τ and Δ_p, overcoming

* Corresponding author.
E-mail addresses: davide.tebaldi@unimore.it (D. Tebaldi), roberto.zanasi@unimore.it (R. Zanasi).

https://doi.org/10.1016/j.sysconle.2025.106164
Received 15 September 2024; Received in revised form 31 March 2025; Accepted 27 May 2025
Available online 17 June 2025

the limitation occurring whenever they are equal to zero and also providing information about the modulus, as well as the phase, of the Nyquist plot in the vicinity of the initial and final points; (4) several results supported by analytical proofs allowing to discriminate the qualitative behavior of the frequency response function in the vicinity of the initial and final points when constructing the qualitative Nyquist plot.

The remainder of this letter is structured as follows. Section 2 introduces the qualitative graphical analysis of the frequency response function, which is deepened in Section 3 and Section 4 by deriving several results for the low and high frequency response, respectively. To validate the proposed results, two case studies are presented in Section 5, while the conclusions are given in Section 6.

2. Qualitative graphical analysis of the frequency response in the complex plane

Consider the transfer function $\bar{G}(s)$ expressed as follows:

$$\bar{G}(s) = \frac{K}{s^h} G(s), \tag{1}$$

where the function $G(s)$ has the following structure:

$$G(s) = \frac{a_m s^m + \cdots + a_3 s^3 + a_2 s^2 + a_1 s + a_0}{b_n s^n + \cdots + b_3 s^3 + b_2 s^2 + b_1 s + b_0} \tag{2}$$

and is characterized by non-null coefficients a_m, b_n, a_0 and b_0, without loss of generality. The initial and final points of the Nyquist plot of function $\bar{G}(s)$ can be obtained by considering the functions $\bar{G}_0(s)$ and $\bar{G}_\infty(s)$, that approximate $\bar{G}(s)$ for $s \simeq 0^+$ and $s \simeq \infty$, respectively. The approximating function $\bar{G}_0(s)$ is obtained from $\bar{G}(s)$ in (1) by neglecting all the terms in s except for the zeros and poles at the origin:

$$\bar{G}_0(s) = \lim_{s \simeq 0^+} \bar{G}(s) = \frac{K}{s^h} G_0, \quad \text{where} \quad G_0 = \frac{a_0}{b_0} \tag{3}$$

and where h is the number of poles of the transfer function $\bar{G}(s)$ at the origin. The approximating function $\bar{G}_\infty(s)$ is deduced from $\bar{G}(s)$ in (1) by considering only the terms in s having the highest degree:

$$\bar{G}_\infty(s) = \lim_{s \simeq \infty} \bar{G}(s) = \frac{K}{s^r} G_\infty, \quad \text{where} \quad G_\infty = \frac{a_m}{b_n} \tag{4}$$

and where $r = h+n-m$ is the relative degree of function $\bar{G}(s)$. The initial point $\bar{P}_0 = \bar{M}_0 e^{j\bar{\varphi}_0}$ and the final point $\bar{P}_\infty = \bar{M}_\infty e^{j\bar{\varphi}_\infty}$ of the Nyquist plot can be computed by considering the magnitude and the phase of the frequency response functions $\bar{G}_0(j\omega)$ and $\bar{G}_\infty(j\omega)$ for $\omega \simeq 0^+$ and $\omega \simeq \infty$:

$$\begin{aligned}
\bar{M}_0 &= \lim_{\omega \simeq 0^+} \frac{|K|}{\omega^h} |G_0| = \begin{cases} \infty & \text{if } h > 0 \\ |K| M_0 & \text{if } h = 0 \\ 0 & \text{if } h < 0 \end{cases}, \quad M_0 = |G_0|, \\
\bar{\varphi}_0 &= \arg(K) - h\frac{\pi}{2} + \varphi_0, \qquad \varphi_0 = \arg(G_0), \\
\bar{M}_\infty &= \lim_{\omega \simeq \infty} \frac{|K|}{\omega^r} |G_\infty| = \begin{cases} 0 & \text{if } r > 0 \\ |K| M_\infty & \text{if } r = 0 \\ \infty & \text{if } r < 0 \end{cases}, \quad M_\infty = |G_\infty|, \\
\bar{\varphi}_\infty &= \arg(K) - r\frac{\pi}{2} + \varphi_\infty, \qquad \varphi_\infty = \arg(G_\infty).
\end{aligned} \tag{5}$$

From (5), it follows that the Nyquist plot starts from the origin when $\omega \simeq 0^+$ if $h < 0$, from a point on the real axis if $h = 0$, or from infinity if $h > 0$, as graphically shown in Fig. 1(a). Dually, from (5) it follows that the Nyquist plot ends at infinity when $\omega \simeq \infty$ if $r < 0$, at a point on the real axis if $r = 0$, or at the origin if $r > 0$, as graphically shown in Fig. 1(b). The initial and final directions of the Nyquist plot are determined by the parameters $\bar{\varphi}_0$ and $\bar{\varphi}_\infty$. However, as shown in Fig. 1, the behavior of the Nyquist curve is not univocal either when $\omega \simeq 0^+$ or $\omega \simeq \infty$, because the system $\bar{G}(s)$ may exhibit a phase lead or a phase lag with respect to the initial and final phases $\bar{\varphi}_0$ and $\bar{\varphi}_\infty$, respectively. This aspect is investigated in detail in the following sections.

Note that the frequency response of function $\bar{G}(s)$ for $s \simeq 0$ and $s \simeq \infty$ is strictly related to the frequency response of function $G(s)$ through (1)–(5). In the following sections, the frequency response analysis of function $G(s)$ is carried out for $s \simeq 0$ and $s \simeq \infty$ to study the behavior in the vicinity of the initial and final points $P_0 = M_0 e^{j\varphi_0}$ and $P_\infty = M_\infty e^{j\varphi_\infty}$. The obtained results can be directly extended to the frequency response of function $\bar{G}(s)$ by using the relations (5) between the initial points $\bar{P}_0$ and P_0 and between the final points $\bar{P}_\infty$ and P_∞.

3. Frequency response of $G(s)$ for $s \simeq 0$

The Taylor series expansion for $s = 0$ of function $G(s)$ in (2) has the following form:

$$G(s) = \sum_{k=0}^{\infty} G_k s^k, \qquad \text{where} \qquad G_k = \frac{1}{k!} \frac{d^k G(s)}{ds^k}\bigg|_{s=0}. \tag{6}$$

From (6), it follows that the frequency response function $G(j\omega)$ of function $G(s)$ can be expressed as follows:

$$G(j\omega) = \sum_{k=0}^{\infty} G_k (j\omega)^k = \underbrace{\sum_{n=0}^{\infty} G_{2n} (-1)^n \omega^{2n}}_{G_{ev}(\omega)} + j\omega \underbrace{\left[\sum_{n=0}^{\infty} G_{2n+1} (-1)^n \omega^{2n}\right]}_{G_{od}(\omega)}, \tag{7}$$

where $G_{ev}(\omega)$ and $\omega G_{od}(\omega)$ are the real and imaginary parts of the frequency response function $G(j\omega)$. Note that the functions $G_{ev}(\omega)$ and $G_{odd}(\omega)$ are only composed of the even and odd coefficients G_k of the Taylor series expansion (6), respectively.

3.1. Sign of the phase $\varphi_0(\omega)$ when $\omega \simeq 0^+$

The phase $\varphi_0(\omega)$ of function $G(j\omega)$ when $\omega \simeq 0^+$ can be expressed from (7) as follows:

$$\begin{aligned}
\varphi_0(\omega) &= \arctan\left[\frac{\omega G_{od}(\omega)}{G_{ev}(\omega)}\right] \\
&= \arctan\left[\frac{\omega(G_1 - G_3\omega^2 + G_5\omega^2 - G_7\omega^6 + \cdots)}{G_0 - G_2\omega^2 + G_4\omega^2 - G_6\omega^6 + \cdots}\right].
\end{aligned} \tag{8}$$

Definition 1. Let parameter Δ_{τ_k} be defined as follows:

$$\Delta_{\tau_k} = (-1)^{\left\lfloor \frac{k}{2} \right\rfloor} \frac{G_k}{G_0}, \tag{9}$$

where $k > 0$ is a positive integer number, and function $\lfloor x \rfloor$ is the floor of x.

Property 1. *Let k be an odd integer index $k \in \{1, 3, 5, \ldots, \infty\}$. If $G_1 = G_3 = G_5 = \cdots = G_{k-2} = 0$, then the phase $\varphi_0(\omega)$ of function $G(j\omega)$ when $\omega \simeq 0^+$ can be approximated as follows:*

$$\varphi_0(\omega) \simeq (-1)^{\frac{k-1}{2}} \frac{G_k}{G_0} \omega^k = \Delta_{\tau_k} \omega^k. \tag{10}$$

Relation (10) holds since $\frac{k-1}{2} = \left\lfloor \frac{k}{2} \right\rfloor$ for odd k.

Proof. The expression of $\varphi_0(\omega)$ in (10) follows directly from (9) and (8) when $\omega \simeq 0^+$ and $G_1 = G_3 = G_5 = \cdots = G_{k-2} = 0$. □

Note that the sign of the parameter Δ_{τ_k} used in (10) determines if the Nyquist plot of the frequency response function $G(j\omega)$ exits the initial point $P_0 = M_0 e^{j\varphi_0}$ defined in (5) by moving clockwise or counter-clockwise in the complex plane, as shown in Fig. 2. Equivalently, the sign of the parameter Δ_{τ_k} used in (10) determines if the Nyquist plot of the frequency response function $\bar{G}(j\omega)$ exits the initial point $\bar{P}_0 = \bar{M}_0 e^{j\bar{\varphi}_0}$ defined in (5) by moving clockwise or counter-clockwise in the complex plane.

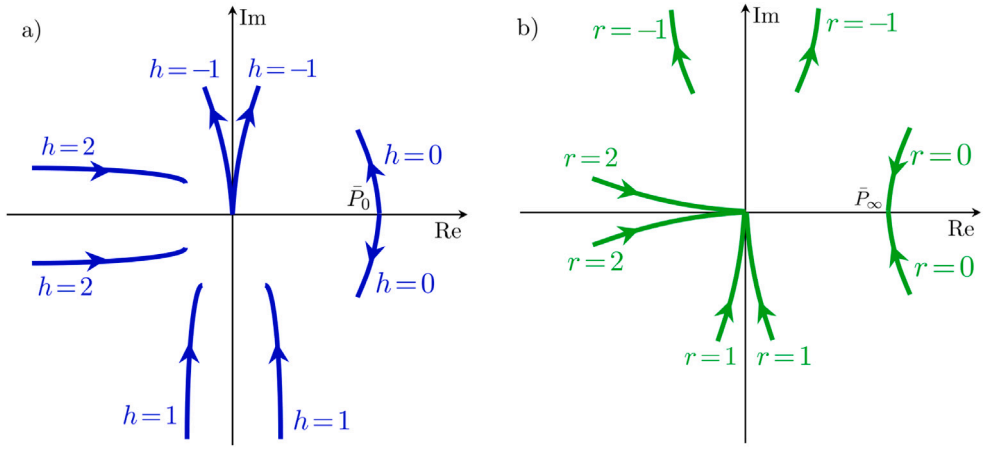

Fig. 1. (a) Nyquist plots in the low frequency range for different values of the number h of poles at the origin and (b) Nyquist plots in the high frequency range for different values of the relative degree r.

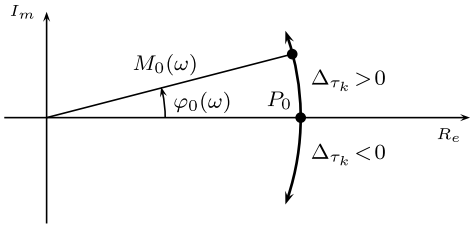

Fig. 2. Nyquist plot of $G(j\omega)$ exiting the initial point P_0 by moving clockwise or counter-clockwise depending on the sign of parameter Δ_{τ_k}.

Definition 2. With reference to the transfer function $G(s)$ defined in (2), let Δ_{ij} denote the following determinant:

$$\Delta_{ij} = \begin{vmatrix} a_i & a_j \\ b_i & b_j \end{vmatrix} = a_i b_j - a_j b_i, \tag{11}$$

for $i, j \in \{0, 1, 2, \dots, n\}$.

Property 2. *All the coefficients G_k present in the series expansion (6), for $k > 0$, can be computed recursively using the following formula:*

$$G_k = \frac{1}{b_0^2}\left(\Delta_{k0} - b_0 \sum_{j=1}^{k-1} G_{k-j} b_j\right). \tag{12}$$

The proof of Property 2 is reported in App. A.

Remark 1. Property 2 provides an elegant and efficient way of computing the coefficients G_k of the Taylor series expansion of a rational transfer function $G(s)$ around the origin in a recursive way, since it does not require to compute the high-order derivatives in the Taylor series expansion coefficients, which may be heavy from a computational point of view.

The recursive formula (12) given in Property 2 can be used for all values of index k. The coefficients G_k for the calculation of the odd coefficients Δ_{τ_k} can equivalently be computed using the recursive formula (13) given in the following Property 3.

Property 3. *All the odd coefficients G_k of the series expansion (6), for $k \in \{1, 3, 5, \dots, \infty\}$, can be computed recursively using the following formula:*

$$G_k = \frac{1}{b_0^2}\left(\nabla_k - \sum_{h=1}^{\frac{k-1}{2}} (-1)^h G_{k-2h} B_h\right), \tag{13}$$

where the coefficients ∇_k are function of the determinants Δ_{ij} defined in (11):

$$\nabla_k = \sum_{j=0}^{\frac{k-1}{2}} (-1)^j \Delta_{k-j,j}, \tag{14}$$

and B_h are polynomials of the coefficients b_k in (2):

$$B_h = b_h^2 + 2\sum_{j=1}^{h} (-1)^j b_{h-j} b_{h+j}. \tag{15}$$

Property 3 can be verified numerically by comparing its results with those of Property 2 for the odd coefficients G_k.

From (11) and (14), it can be observed that the coefficients ∇_k are function only of the parameters a_i and b_i of $G(s)$ in (2) characterized by indexes $i \le k$.

Theorem 1. *The sign of the phase $\varphi_0(\omega)$ of function $G(j\omega)$ when $\omega \simeq 0^+$ can be determined as follows:*

$$sign(\varphi_0(\omega)) = sign(\Delta_{\tau_k}), \tag{16}$$

where Δ_{τ_k}, defined in (9), is the first non-zero element of the series of odd coefficients Δ_{τ_k} for increasing values of the odd index $k \in \{1, 3, 5, \dots, \infty\}$. Furthermore, the coefficients Δ_{τ_k} in (16) can also be expressed as follows:

$$\Delta_{\tau_k} = (-1)^{\frac{k-1}{2}} \frac{\nabla_k}{a_0 b_0}. \tag{17}$$

Proof. The first equality $sign(\varphi(\omega)) = sign(\Delta_{\tau_k})$ in (16) comes directly from (10) in Property 1 and from Definition 1 of Δ_{τ_k} in (9). Then, from (13) it follows that when $G_1 = G_3 = G_5 = \cdots = G_{k-2} = 0$, the coefficients G_k can be expressed as follows:

$$G_k = \frac{\nabla_k}{b_0^2}. \tag{18}$$

Therefore, substituting (18) in (9) and recalling the static gain $G_0 = a_0/b_0$ from (5), yield the expression of Δ_{τ_k} in (17). □

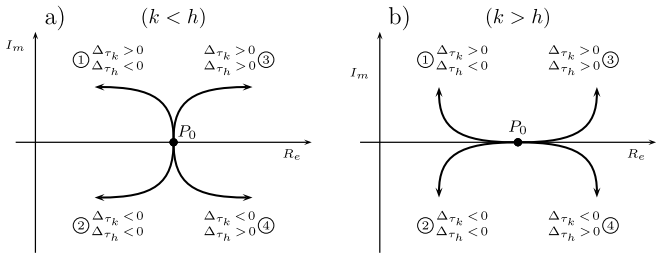

Fig. 3. Different types of Nyquist plots when exiting the initial point P_0.

3.2. Behavior of the modulus $M_0(\omega)$ when $\omega \simeq 0^+$

Theorem 2. *The modulus $M_0(\omega)$ of function $G(j\omega)$ when $\omega \simeq 0^+$ increases or decreases as follows:*

$$\begin{aligned} &M_0(\omega) \text{ increases if } \Delta_{\tau_k} > 0, \\ &M_0(\omega) \text{ decreases if } \Delta_{\tau_k} < 0, \end{aligned} \tag{19}$$

where Δ_{τ_k} is the first non-zero element of the series of even coefficients Δ_{τ_k} for increasing values of the even index $k \in \{0, 2, 4, \dots, \infty\}$.

Proof. When $\omega \simeq 0^+$, from (7) it follows that the modulus of $G(j\omega)$ can be approximated as follows:

$$M_0(\omega) \simeq |G_{ev}(\omega)| \simeq |G_0| \left| 1 - \frac{G_2}{G_0}\omega^2 + \frac{G_4}{G_0}\omega^4 - \frac{G_6}{G_0}\omega^6 + \cdots \right|, \tag{20}$$

where $G_{ev}(\omega)$ is the real part of $G(j\omega)$. Note that the modulus $M_0(\omega)$ of point $G(j\omega)$ when $\omega \simeq 0^+$ contains only the even coefficients G_k, for $k \in \{0, 2, 4, \dots, \infty\}$, of the series expansion (6). From (20), it can be observed that when $\omega \simeq 0^+$ the modulus $|G(j\omega)|$ increases or decreases depending on the sign of the coefficients $-\frac{G_2}{G_0}$, $\frac{G_4}{G_0}$, $-\frac{G_6}{G_0}$, etc. Replacing Definition 1 of Δ_{τ_k} from (9) in (20) yields (19). □

Remark 2. Consider the transfer function:

$$G_T(s) = G(s)\,T(s) = G(s)\,e^{-t_0 s}, \tag{21}$$

where $G(s)$ is defined in (2) and $T(s) = e^{-t_0 s}$ is the transfer function of a time delay. Recalling that $\arg(e^{-jt_0\omega}) = -t_0\omega$, and using (10), the phase $\varphi_{T_0}(\omega)$ of function $G_T(j\omega)$ when $\omega \simeq 0^+$ can be approximated as follows:

$$\varphi_{T_0}(\omega) \simeq (\Delta_{\tau_k}\,\omega^{k-1} - t_0)\omega. \tag{22}$$

From (22), it follows that relation (16) in this case can be rewritten as follows:

$$\text{sign}(\varphi_{T_0}(\omega)) = \begin{cases} \text{sign}(\Delta_{\tau_k} - t_0) & \text{if } k = 1, \\ < 0 & \text{if } k > 1, \end{cases}$$

where the last condition holds since $\Delta_{\tau_k}\,\omega^{k-1} \simeq 0$ when $\omega \simeq 0$ and $k > 1$, and $t_0 > 0$ is the time delay in the system. Conversely, relation (19) remains unchanged since $|e^{-jt_0\omega}| = 1$.

3.3. Exiting the initial point P_0 when $\omega \simeq 0^+$

Theorems 1 and 2 have shown that the odd coefficients G_1, G_3, G_5, … and the even coefficients G_2, G_4, G_6, … in (6) can be used to determine the sign of the phase $\varphi_0(\omega)$ and whether the modulus $M_0(\omega)$ increases or decreases when $\omega \simeq 0^+$. The combined results of Theorems 1 and 2 allow to determine how the frequency response function $G(j\omega)$ exits the initial point P_0 when $\omega \simeq 0^+$. Specifically, the following two Lemmas originate from Theorem 1.

Lemma 1. *When $\omega \simeq 0^+$ and the first non-zero odd parameter Δ_{τ_k} has an index $k < h$, where h is the index of the first not-zero even parameter Δ_{τ_h}, the function $G(j\omega)$ exits the initial point P_0 by moving in the complex plane along a direction* perpendicular *to the real axis. The possible four Nyquist curves that can be obtained are shown in Fig. 3(a).*

Proof. From (7) and (9), if $\omega \simeq 0^+$, $\Delta_{\tau_k} \neq 0$ is the first non-zero odd parameter, and $\Delta_{\tau_h} \neq 0$ is the first non-zero even parameter, it follows that function $G(j\omega)$ can be expressed as:

$$G(j\omega) \simeq G_0 - G_h\omega^h + jG_k\omega^k \simeq G_0(1 + \Delta_{\tau_h}\omega^h + j\Delta_{\tau_k}\omega^k). \tag{23}$$

From (23) it follows that, when $\omega \simeq 0^+$, the function $G(j\omega)$ exits the initial point P_0 by drawing a Nyquist curve that moves along a direction which is *perpendicular* to the real axis because the infinitesimal $\Delta_{\tau_k}\,\omega^k$ is larger than the infinitesimal $\Delta_{\tau_h}\omega^h$, since $k < h$. □

The four possible Nyquist curves shown in Fig. 3(a) depend on the positive or negative values of the two parameters Δ_{τ_k} and Δ_{τ_h}.

Lemma 2. *When $\omega \simeq 0^+$ and the first non-zero odd parameter Δ_{τ_k} has an index $k > h$, where h is the index of the first not-zero even parameter Δ_{τ_h}, the function $G(j\omega)$ exits the initial point P_0 by drawing a Nyquist curve that moves along a direction* parallel *to the real axis. The Nyquist curves that can be obtained in this case are shown in Fig. 3(b).*

Proof. From (7) and (9), when $\omega \simeq 0^+$, $\Delta_{\tau_k} \neq 0$ is the first non-zero odd parameter, and $\Delta_{\tau_h} \neq 0$ is the first non-zero even parameter, it follows that function $G(j\omega)$ can be expressed as in (23). In this case, from (23) it follows that, when $\omega \simeq 0^+$, the function $G(j\omega)$ exits the initial point P_0 by drawing a Nyquist curve that moves along a direction which is *parallel* to the real axis because the infinitesimal $\Delta_{\tau_k}\,\omega^k$ is smaller than the infinitesimal $\Delta_{\tau_h}\omega^h$, since $k > h$. □

In this case, the four possible Nyquist curves are shown in Fig. 3(b).

4. Frequency response of $G(s)$ at $s \simeq \infty$

Substituting $\tilde{s} = \frac{1}{s}$ in (1) yields:

$$\tilde{G}(s) = \frac{K}{s^r}\,\tilde{G}(s), \qquad \text{where} \qquad r = h + n - m \tag{24}$$

is the relative degree of function $\tilde{G}(s)$ and function $\tilde{G}(s)$ is:

$$\tilde{G}(s) = \frac{(a_0\tilde{s}^m + a_1\tilde{s}^{m-1} + \cdots + a_{m-2}\tilde{s}^2 + a_{m-1}\tilde{s} + a_m)}{(b_0\tilde{s}^n + b_1\tilde{s}^{n-1} + \cdots + b_{n-2}\tilde{s}^2 + b_{n-1}\tilde{s} + b_n)}. \tag{25}$$

Function $\tilde{G}(s)$ has a similar structure as function $G(s)$ in (2), in which the coefficients a_i and b_i are in reversed order.

Definition 3. Let $\tilde{a}_i$ and $\tilde{b}_j$ denote the "dual version" of coefficients a_i and b_j, defined as follows:

$$\tilde{a}_i = a_{m-i} \qquad \text{and} \qquad \tilde{b}_j = b_{n-j}, \tag{26}$$

for $i \in \{1, 2, \dots, m\}$ and $j \in \{1, 2, \dots, n\}$. From (26), it follows that:

$$a_i = \tilde{a}_{m-i} \qquad \text{and} \qquad b_j = \tilde{b}_{n-j}. \tag{27}$$

Substituting (27) in (25) yields:

$$\tilde{G}(s) = \frac{(\tilde{a}_m\,\tilde{s}^m + \tilde{a}_{m-1}\,\tilde{s}^{m-1} + \cdots + \tilde{a}_2\,\tilde{s}^2 + \tilde{a}_1\,\tilde{s} + \tilde{a}_0)}{(\tilde{b}_n\,\tilde{s}^n + \tilde{b}_{n-1}\,\tilde{s}^{n-1} + \cdots + \tilde{b}_2\,\tilde{s}^2 + \tilde{b}_1\,\tilde{s} + \tilde{b}_0)}, \tag{28}$$

having now the same structure as function $G(s)$ in (2) but using the dual coefficients $\tilde{a}_i$ and $\tilde{b}_j$ and the new variable $\tilde{s}$.

The frequency response of function $G(s)$ at $s \simeq \infty$ can be studied using the Taylor series expansion of $\tilde{G}(s)$ at $\tilde{s} = 0$:

$$\tilde{G}(s) = \sum_{k=0}^{\infty} \tilde{G}_k\,\tilde{s}^k = \tilde{G}_0 + \tilde{G}_1\tilde{s} + \tilde{G}_2\tilde{s}^2 + \cdots, \tag{29}$$

where the coefficients $\tilde{G}_k$ in (29) are the dual version of the coefficients G_k in (6) using (26). Equivalently, also the coefficients Δ_{τ_k} in (9), Δ_{ij} in (11), ∇_k in (14) and B_h in (15) can be dualized into $\tilde{\Delta}_{\tau_k}$, $\tilde{\Delta}_{ij}$, $\tilde{\nabla}_k$ and $\tilde{B}_h$ using (26). In particular, the dual determinant $\tilde{\Delta}_{ij}$ is defined as follows:

$$\tilde{\Delta}_{ij} = \begin{vmatrix} a_{m-i} & a_{m-j} \\ b_{n-i} & b_{n-j} \end{vmatrix} = a_{m-i}b_{n-j} - a_{m-j}b_{n-i}. \tag{30}$$

Note that $\tilde{G}_0 = \frac{a_m}{b_n}$ in (29) is equal to G_∞ defined in (4).

Theorem 3 (*Dual of Theorem 1*). *The sign of the phase $\varphi_\infty(\omega)$ of function $G(j\omega)$ when $\omega \simeq \infty$ can be determined as follows:*

$$sign(\varphi_\infty(\omega)) = sign(-\tilde{\Delta}_{\tau_k}), \tag{31}$$

where $\tilde{\Delta}_{\tau_k}$ is the first non-zero element of the series of odd coefficients $\tilde{\Delta}_{\tau_k}$, for increasing values of the odd index $k \in \{1, 3, 5, \dots, \infty\}$. Furthermore, the coefficient $\tilde{\Delta}_{\tau_k}$ in (31) can also be expressed as follows:

$$\tilde{\Delta}_{\tau_k} = (-1)^{\left\lfloor \frac{k}{2} \right\rfloor} \frac{\tilde{\nabla}_k}{a_m b_n}. \tag{32}$$

Proof. The frequency response $\tilde{G}(j\omega)$ of function $\tilde{G}(s)$ in (29) when $\omega \simeq \infty$ can be expressed as follows:

$$\begin{aligned} \tilde{G}(j\omega) &= \sum_{k=0}^{\infty} \tilde{G}_k \frac{1}{(j\omega)^k} = \sum_{k=0}^{\infty} \tilde{G}_k \frac{(-j)^k}{\omega^k} \\ &= \tilde{G}_0 - \frac{\tilde{G}_2}{\omega^2} + \frac{\tilde{G}_4}{\omega^4} + \cdots - \frac{j}{\omega}\left[\tilde{G}_1 - \frac{\tilde{G}_3}{\omega^2} + \frac{\tilde{G}_5}{\omega^4} + \dots\right]. \end{aligned} \tag{33}$$

When $\omega \simeq \infty$ and $\tilde{G}_1 = \tilde{G}_3 = \tilde{G}_5 = \cdots = \tilde{G}_{k-2} = 0$, the phase $\varphi_\infty(\omega)$ of $\tilde{G}(j\omega)$ in (33) and, equivalently, of $G(j\omega)$, can be approximated as follows:

$$\varphi_\infty(\omega) \simeq \arctan\left[-\frac{(-1)^{\left\lfloor \frac{k}{2} \right\rfloor}\tilde{G}_k}{\tilde{G}_0\,\omega^k}\right] \simeq \frac{-\tilde{\Delta}_{\tau_k}}{\omega^k}, \tag{34}$$

from which equality (31) follows. Finally, the expression (32) is the dual version of (17) in Theorem 1. □

Theorem 4 (*Dual of Theorem 2*). *The modulus $M_\infty(\omega)$ of function $G(j\omega)$ when $\omega \simeq \infty$ increases or decreases as follows:*

$$\begin{aligned} &M_\infty(\omega) \quad \textit{increases if} \quad \tilde{\Delta}_{\tau_k} > 0, \\ &M_\infty(\omega) \quad \textit{decreases if} \quad \tilde{\Delta}_{\tau_k} < 0, \end{aligned} \tag{35}$$

where $\tilde{\Delta}_{\tau_k}$ is the first non-zero element of the series of even coefficients $\tilde{\Delta}_{\tau_k}$ for increasing values of the even index $k \in \{0, 2, 4, \dots, \infty\}$.

Proof. When $\omega \simeq \infty$, from (33) it follows that $|\tilde{G}(j\omega)|$ and, equivalently, $M_\infty(\omega)$ can be expressed as:

$$M_\infty(\omega) = |\tilde{G}(j\omega)| \simeq |\tilde{G}_0| \left|1 - \frac{\tilde{G}_2}{\tilde{G}_0\omega^2} + \frac{\tilde{G}_4}{\tilde{G}_0\omega^4} - \frac{\tilde{G}_6}{\tilde{G}_0\omega^6} + \cdots\right|, \tag{36}$$

which is the dual of $M_0(\omega)$ in (20). Therefore, the same proof as Theorem 2 applies here using the dual coefficients $\tilde{\Delta}_{\tau_k}$. □

Remark 3. When $\omega \simeq \infty$, the final part of the Nyquist diagram of function $G_T(j\omega)$ in (21) makes infinite clockwise rotations around its final point P_{T_∞}, since $\arg(e^{-jt_0\omega}) = -t_0\omega \simeq -\infty$ when $\omega \simeq \infty$. Therefore, in this case, it is not of interest to further analyze the behavior of function $G_T(j\omega)$ when $\omega \simeq \infty$ from a qualitative point of view.

4.1. Entering the final point P_∞ when $\omega \simeq \infty$

Following the same outline of Section 3.3, the following Lemmas 3 and 4, which are the dual of Lemmas 1 and 2, respectively, originate from Theorem 3.

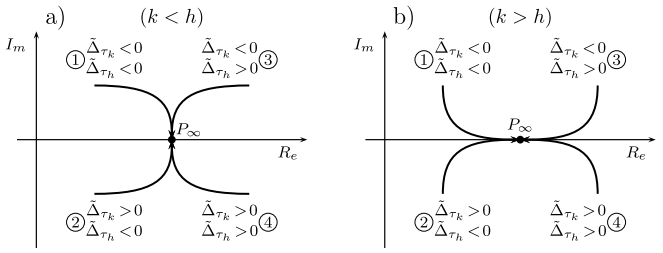

Fig. 4. Different types of Nyquist plots when entering the final point P_∞.

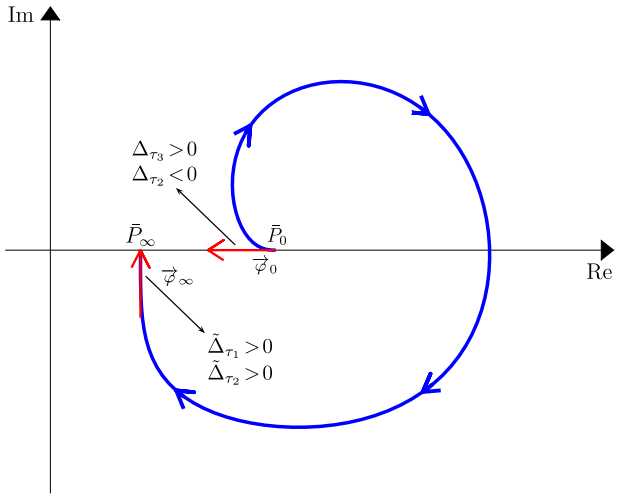

Fig. 5. Qualitative Nyquist plot of $G(j\omega)$ associated with $G(s)$ in (37).

Lemma 3. *(Dual of Lemma 1) When $\omega \simeq \infty$ and the first non-zero odd parameter $\tilde{\Delta}_{\tau_k}$ has an index $k < h$, where h is the index of the first not-zero even parameter $\tilde{\Delta}_{\tau_h}$, the function $G(j\omega)$ enters the final point P_∞ by drawing a Nyquist curve that moves along a direction* perpendicular *to the real axis.*

From Lemma 3 and Theorem 4 it follows that, when $\omega \simeq \infty$ and $k < h$, the function $G(j\omega)$ enters the final point P_∞ by drawing one of the four Nyquist curves shown in Fig. 4(a).

Lemma 4. *(Dual of Lemma 2) When $\omega \simeq \infty$ and the first non-zero odd parameter $\tilde{\Delta}_{\tau_k}$ has an index $k > h$, where h is the index of the first not-zero even parameter $\tilde{\Delta}_{\tau_h}$, the function $G(j\omega)$ enters the final point P_∞ by drawing a Nyquist curve that moves along a direction* parallel *to the real axis.*

From Lemma 4 and Theorem 4 it follows that, when $\omega \simeq \infty$ and $k > h$, the function $G(j\omega)$ enters the final point P_∞ by drawing one of the four Nyquist curves shown in Fig. 4(b).

5. Case studies

5.1. First case study

Reference is made to the following transfer function:

$$\bar{G}(s) = \frac{2s^3 + 6s^2 + 2s + 1}{4s^3 + 5s^2 + 2s + 1}. \tag{37}$$

The initial and final points $\bar{P}_0$ and $\bar{P}_\infty$ of the Nyquist plot of $\bar{G}(j\omega)$ are characterized by: $\bar{M}_0 = 1$, $\bar{M}_\infty = 0.5$, $\bar{\varphi}_0 = \bar{\varphi}_\infty = 0$. Applying Definition

1 and Property 2 yields:

$$\Delta_{\tau_1} = \frac{G_1}{G_0} = 0, \quad \Delta_{\tau_2} = -\frac{G_2}{G_0} = -1, \quad \Delta_{\tau_3} = -\frac{G_3}{G_0} = 4,$$
$$\tilde{\Delta}_{\tau_1} = \frac{\tilde{G}_1}{\tilde{G}_0} = \frac{7}{4}, \qquad \tilde{\Delta}_{\tau_2} = -\frac{\tilde{G}_2}{\tilde{G}_0} = \frac{27}{16}.$$

Remark 4. The procedure described in [18] did not consider in detail the case in which the parameter called Δ_τ, which is Δ_{τ_1} in this letter, was equal to zero, because of the complexity of the calculations. Therefore, the procedure in [18] would fail to discriminate the behavior of the phase $\varphi_0(\omega)$ of $\bar{G}(j\omega)$ when $\omega \simeq 0^+$ in this case. On the contrary, the detailed frequency analysis performed in this letter always allows to discriminate the behavior of the phase $\varphi_0(\omega)$ when $\omega \simeq 0^+$ thanks to Theorem 1, and recalling that the parameters Δ_{τ_k} can be effectively computed using Definition 1 and Property 2. Furthermore, it is also possible to discriminate the direction of the function $\bar{G}(j\omega)$ in the complex plane when exiting the initial point $\bar{P}_0$ thanks to Lemmas 1 and 2, as well as to discriminate the behavior of the modulus $M_0(\omega)$ when $\omega \simeq 0^+$ thanks to Theorem 2.

Applying Theorems 1 and 2, since $\Delta_{\tau_3} > 0$, $\Delta_{\tau_2} < 0$ (case $k > h$), the Nyquist plot exits the initial point $\bar{P}_0$ as the curve ① in Fig. 3(b), as shown in Fig. 5.

Remark 5. The behavior of the phase $\varphi_\infty(\omega)$ when $\omega \simeq \infty$ can be discriminated thanks to Theorem 3, and recalling that the parameters $\tilde{\Delta}_{\tau_k}$ can be effectively computed using Definition 1 and Property 2. Furthermore, it is also possible to discriminate the direction of the function $\bar{G}(j\omega)$ in the complex plane when entering the final point $\bar{P}_\infty$ thanks to Lemmas 3 and 4, as well as to discriminate the behavior of the modulus $M_\infty(\omega)$ when $\omega \simeq \infty$ thanks to Theorem 4.

Applying Theorems 3 and 4, since $\tilde{\Delta}_{\tau_1} > 0$, $\tilde{\Delta}_{\tau_2} > 0$ (case $k < h$), the Nyquist plot enters the final point $\bar{P}_\infty$ as the curve ④ in Fig. 4(a), as shown in Fig. 5.

The qualitative behavior of the remaining part of the Nyquist plot when $\omega \neq 0^+$ and $\omega \neq \infty$ can be determined by calculating the intersections with the real axis using the Routh–Hurwitz criterion. The red arrows in Fig. 5 denote the following vectors:

$$\overrightarrow{\varphi}_0 = \left.\frac{d\bar{G}(j\omega)}{d\omega}\right|_{\omega\simeq 0^+} \quad \text{and} \quad \overrightarrow{\varphi}_\infty = \left.\frac{d\bar{G}(j\omega)}{d\omega}\right|_{\omega\simeq\infty}$$

indicating the direction tangential to the Nyquist plot at the initial and final points.

5.2. Second case study

Reference is made to the following transfer function:

$$\bar{G}(s) = \frac{s^2 + 12s + 35}{s(s^4 + 12s^3 + 30s^2 + 28s + 9)}. \tag{38}$$

Applying Definition 1 and Property 2 yields:

$$\Delta_{\tau_1} = \frac{G_1}{G_0} = -2.76, \quad \tilde{\Delta}_{\tau_1} = \frac{\tilde{G}_1}{\tilde{G}_0} = 0, \quad \tilde{\Delta}_{\tau_3} = -\frac{\tilde{G}_3}{\tilde{G}_0} = 88.$$

Applying Theorem 1, since $\Delta_{\tau_1} < 0$, the Nyquist plot starts by lagging with respect to the initial phase $\bar{\varphi}_0$, as shown in Fig. 6.

Remark 6. The procedure described in [18] did not consider in detail the case in which the parameter called Δ_p, which is $\tilde{\Delta}_{\tau_1}$ in this letter, was equal to zero, because of the complexity of the calculations. Therefore, the procedure in [18] would fail to discriminate the phase of $\bar{G}(j\omega)$ when $\omega \simeq \infty$ in this case. On the contrary, the detailed frequency analysis performed in this letter always allows to discriminate the behavior thanks to Theorem 3 and recalling that the parameters $\tilde{\Delta}_{\tau_k}$ can be effectively computed using Definition 1 and Property 2.

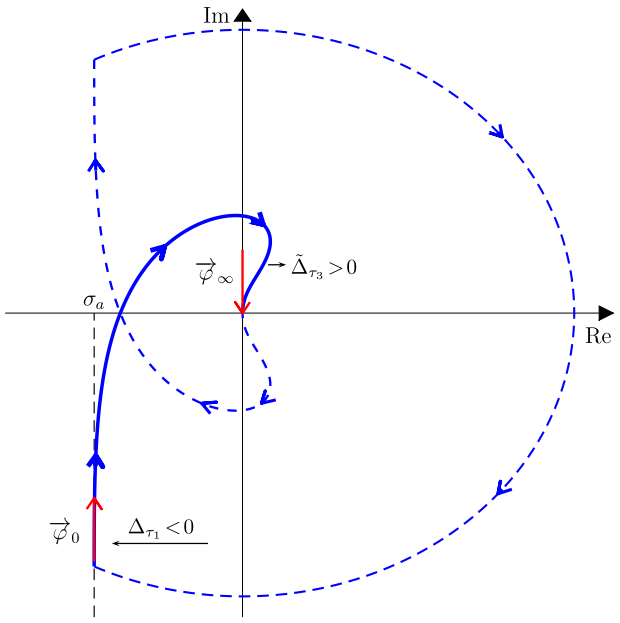

Fig. 6. Qualitative Nyquist plot of $G(j\omega)$ associated with $G(s)$ in (38).

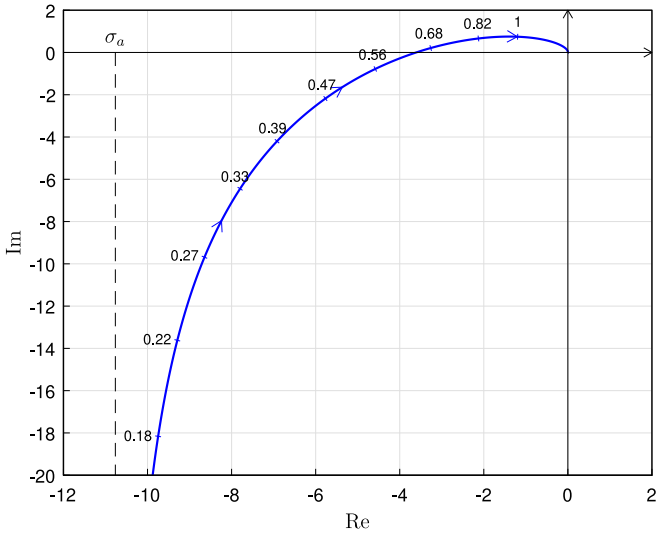

Fig. 7. Actual Nyquist plot of $G(j\omega)$ associated with $G(s)$ in (38).

Applying Theorem 3, since $\tilde{\Delta}_{\tau_1} = 0$ and $\tilde{\Delta}_{\tau_3} > 0$, the Nyquist plot ends by lagging with respect to the final phase $\bar{\varphi}_\infty$, as shown in Fig. 6.

The qualitative behavior of the remaining part of the Nyquist curve when $\omega \neq 0^+$ and $\omega \neq \infty$ can be determined by calculating the intersections with the real axis using the Routh–Hurwitz criterion and abscissa σ_a of the asymptote shown in Fig. 6.

The actual Nyquist plot is shown in Fig. 7. By comparing Figs. 6 and 7, it can be observed that qualitative representations of Nyquist plots are much more effective in providing a global view of the frequency response function both at low and high frequency. Furthermore, Fig. 6 shows that qualitative Nyquist plots make it easier to construct the complete diagram in order to perform a stability analysis.

6. Conclusion

This letter has addressed the graphical analysis of the frequency response function, with the objective of improving the procedure for the qualitative construction of Nyquist plots. Several analytical results have been derived and proven, concerning the graphical behavior of the frequency response function at low and high frequency. Two case studies have been considered, showing how the obtained results allow to discriminate the qualitative behavior of the frequency response on the Nyquist plot in the vicinity of the initial and final points. The future directions of this work include the possible further generalization of the proposed procedure, in order to include a larger class of irrational transfer functions.

CRediT authorship contribution statement

Davide Tebaldi: Writing – review & editing, Writing – original draft, Visualization, Software, Resources, Methodology, Investigation, Formal analysis, Data curation, Conceptualization. **Roberto Zanasi:** Writing – review & editing, Writing – original draft, Visualization, Software, Resources, Methodology, Investigation, Formal analysis, Data curation, Conceptualization.

Funding

The work was partly supported by the University of Modena and Reggio Emilia through the action FARD (Finanziamento Ateneo Ricerca Dipartimentale) 2023/2024, and funded under the National Recovery and Resilience Plan (NRRP), Mission 04 Component 2 Investment 1.5 - NextGenerationEU, Call for tender n. 3277 dated 30/12/2021 Award Number: 0001052 dated 23/06/2022.

Declaration of competing interest

The authors declare that they have no known competing financial interests or personal relationships that could have appeared to influence the work reported in this paper.

Appendix. Proof of Property 2

Proof. The formula for computing the k-th derivative of the quotient of two functions, that are the numerator $N(s)$ and the denominator $D(s)$ of the transfer function $G(s)$ in (2) in this case, is known from the literature [19]. Using (2), the following hold:

$$\left.\frac{d^k N(s)}{ds^k}\right|_{s=0} = k!\, a_k \quad \text{and} \quad \left.\frac{d^k D(s)}{ds^k}\right|_{s=0} = k!\, b_k. \tag{A.1}$$

Using (A.1) and the formula for computing the k-th derivative of the quotient of two functions in [19], the coefficients G_k in (6) can be computed as follows:

$$\begin{aligned} G_k = \frac{1}{k!}\left.\frac{d^k G(s)}{ds^k}\right|_{s=0} &= \frac{1}{k!\, b_0}\left(k!\, a_k - k! \sum_{i=1}^{k} b_{k+1-i} \underbrace{\frac{\left.\frac{d^{(i-1)}G(s)}{ds^{(i-1)}}\right|_{s=0}}{(i-1)!}}_{G_{i-1}} \right), \\ &= \frac{1}{b_0^2}\left(a_k b_0 - b_0 \sum_{i=1}^{k} b_{k+1-i}\, G_{i-1} \right). \end{aligned} \tag{A.2}$$

Using $j = k + 1 - i$, the last equation of (A.2) can be rewritten as follows:

$$G_k = \frac{1}{b_0^2}\left(\underbrace{a_k\, b_0 - a_0 b_k}_{\Delta_{k0}} - b_0 \sum_{j=1}^{k-1} b_j G_{k-j} \right), \tag{A.3}$$

which coincides with (12). □

Data availability

No data was used for the research described in the article.

References

[1] G.F. Franklin, J.D. Powell, A. Emami-Naeini, Feedback Control of Dynamic Systems, fourth ed., Prentice Hall PTR, Upper Saddle River, NJ, USA, 2001.
[2] A.G.J. MacFarlane, H. Nyquist, Frequency-Response Methods in Control Systems, IEEE Comput. Soc. Press, New York, NY, USA, 1979.
[3] Y.-L. Zhang, M. Zhu, D. Li, J.-M. Wang, Static boundary feedback stabilization of an anti-stable wave equation with both collocated and non-collocated measurements, Systems Control Lett. 154 (2021) 104967.
[4] M. Bucolo, A. Buscarino, L. Fortuna, M. Frasca, Nyquist plots for MIMO systems under frequency transformations, IEEE Control. Syst. Lett. 6 (2022) 169–174.
[5] A. Buscarino, L. Fortuna, M. Frasca, Nyquist plots under frequency transformations, Systems Control Lett. 125 (2019) 16–21.
[6] H. Khalil, Nonlinear Systems, Prentice Hall PTR, 2002.
[7] K.J. Astrom, R.M. Murray, Feedback Systems: An Introduction for Scientists and Engineers, Princeton University Press, Princeton, NJ, USA, 2008.
[8] R. Zanasi, S. Cuoghi, L. Ntogramatzidis, Analytical design of lead-lag compensators on Nyquist and Nichols planes, IFAC Proc. Vol. 44 (1) (2011) 7666–7671.
[9] F. Zhang, et al., Swallowing events recognition method based on complex impedance pharyngography and nyquist plots, IEEE Sensors J. 22 (18) (2022) 18076–18084.
[10] P. Kawka, G. De Mey, B. Vermeersch, Thermal characterization of electronic packages using the nyquist plot of the thermal impedance, IEEE Trans. Compon. Packag. Technol. 30 (4) (2007) 660–665.
[11] Y.Z. Tan, C.K. Pang, Relaxing LMI conservatism using nyquist plots and its application to robust mechatronics synthesis, IEEE Trans. Control Syst. Technol. 25 (2) (2017) 600–610.
[12] A. Emami-Naeini, The shapes of Nyquist plots [lecture notes], IEEE Control Syst. Mag. 29 (5) (2009) 102–115.
[13] Control system toolbox documentation, 2024, https://it.mathworks.com/products/control.html. (Last Accessed September 2024).
[14] LabVIEW documentation, 2024, https://www.ni.com/en/shop/labview.html. (Last Accessed September 2024).
[15] T. Andresen, A logarithmic-amplitude polar diagram, Model. Identif. Control 22 (2) (2001) 65–72.
[16] B.C. Kuo, F. Golnaraghi, Automatic Control Systems, ninth ed., John Wiley & Sons, Inc., New York, NY, USA, 2002.
[17] R.C. Dorf, R.H. Bishop, Modern Control Systems, eleventh ed., Prentice Hall PTR, Upper Saddle River, NJ, USA, 2008.
[18] R. Zanasi, F. Grossi, L. Biagiotti, Qualitative graphical representation of Nyquist plots, Systems Control Lett. 83 (2015) 53–60.
[19] C. Xenophontos, A formula for the nth derivative of the quotient of two functions, 2021, arXiv preprint, arXiv:2110.09292v1. [Online]. Disponibile su: https://arxiv.org/abs/2110.09292.